The Astrophysical Journal, 647: L25–L28, 2006 August 10

THE STELLAR HALO AND OUTER DISK OF M33

Alan W. McConnachie,[1] Scott C. Chapman,[1,2] Rodrigo A. Ibata,[3] Annette M. N. Ferguson,[4] Mike J. Irwin,[5] Geraint F. Lewis,[6] Nial R. Tanvir,[7] and Nicolas Martin[3]

Received 2006 May 9; accepted 2006 June 29; published 2006 July 31

ABSTRACT

We present first results from a Keck DEIMOS spectroscopic survey of red giant branch (RGB) stars in M33. The radial velocity distributions of the stars in our fields are well described by three Gaussian components, corresponding to a candidate halo component with an uncorrected radial velocity dispersion of $\sigma \simeq 50$ km s^{-1}, a candidate disk component with a dispersion $\sigma \simeq 16$ km s^{-1}, and a third component offset from the disk by $\sim$50 km s^{-1}, but for which the dispersion is not well constrained. By comparing our data to a model of M33 based on its H I rotation curve, we find that the stellar disk is offset in velocity by $\sim$25 km s^{-1} from the H I disk, consistent with the warping that exists between these components. The spectroscopic metallicity of the halo component is [Fe/H] $\simeq -1.5$, significantly more metal-poor than the implied metallicity of the disk population ([Fe/H] $\simeq -0.9$), which also has a broader color dispersion than the halo population. These data represent the first detections of individual stars in the halo of M33 and, despite being $\sim$10 times less massive than M31 or the Milky Way, all three of these disk galaxies have stellar halo components with a similar metallicity. The color distribution of the third component is different from the disk and the halo but is similar to that expected for a single, coeval, stellar population, and could represent a stellar stream. More observations are required to determine the true nature of this intriguing third kinematic component in M33.

Subject headings: galaxies: individual (M33) — galaxies: stellar content — galaxies: structure — Local Group

Online material: color figures

1. INTRODUCTION

M33, the Triangulum galaxy (R.A. = $1^h33^m51^s$, decl. = 30°39′36″), is the third brightest Local Group galaxy, with an integrated luminosity of $M_V = -18.9$. It is a late-type spiral, Sc II–III, with two open spiral arms and no clear evidence of any bulge component (Bothun 1992; Minniti et al. 1993; McLean & Liu 1996). The overwhelming majority of light in M33 is distributed in an exponential disk component (de Vaucouleurs 1959), and the optical disk is tilted at nearly 30° to the strongly warped H I envelope (Rogstad et al. 1976). The mass-to-light ratio of its nucleus is small ($M/L < 0.4$), ruling out the presence of a supermassive black hole (Kormendy & McClure 1993; Lauer et al. 1998) like that implied to exist in the Milky Way (MW; Genzel et al. 1997) and M31 (Dressler & Richstone 1988; Kormendy 1988).

Chandar et al. (2002) analyze the kinematics of stars clusters in M33 and find two distinct kinematic populations, which they argue represent a disk and halo population, although individual stars belonging to a halo component in M33 had not been directly observed.[8] In a companion paper by A. Ferguson et al. (2006, in preparation; see also Ferguson et al. 2006), we present our wide field photometry of this galaxy taken with the Isaac Newton Telescope Wide Field Camera (INT WFC) and show that a low-level stellar component dominates the radial profile of M33 at large radius, implying the presence of an extended stellar halo in M33. Unlike its massive neighbor, M31, there is no evidence of substructure in M33 to a surface brightness threshold of $\mu_V \simeq 30$ mag arcsec^2.

In this Letter we present first results from a spectroscopic survey of red giant branch (RGB) stars in M33 using the Deep Imaging Multi-Object Spectrograph (DEIMOS) on Keck II (Faber et al. 2003). Section 2 describes our observations. Section 3 analyzes the radial velocity distributions in our fields. Section 4 analyzes the metallicities of our target stars, and § 5 discusses our results and concludes. We assume a distance to M33 of 809 ± 24 kpc (McConnachie et al. 2004a, 2005).

2. OBSERVATIONS

Since 2002 our group has been conducting a spectroscopic survey of M31 using DEIMOS on Keck II (Ibata et al. 2004, 2005; McConnachie et al. 2004b; Chapman et al. 2005, 2006). In 2005 September–October we extended the scope of this survey to M33. The two fields analyzed here were taken at the end of the night at high air mass, during imperfect weather conditions. Their location relative to the disk of M33 can be seen in Figure 1 and are positioned $\sim$38′ (9 kpc) along the southern major axis to study the kinematics of stars at the edge of the M33 disk. In the same way as in our M31 study, we used the "minislitlet" DEIMOS setup for these fields, which significantly increases the multiplexing capabilities of this instrument (Ibata et al. 2005; Chapman et al. 2006). Targets were selected from the INT survey using a color-magnitude box defined by $20.5 < i < 22.0$ and $1.0 < (V - i)_0 < 4.0$. Other targets brighter than $i = 22$ were automatically chosen to fill in the available space of the spectrograph detector.

[1] Department of Physics and Astronomy, University of Victoria, Victoria, BC V8P 1A1, Canada; alan@uvic.ca.

[2] California Institute of Technology, Pasadena, CA 91125; schapman@submm.caltech.edu.

[3] Observatoire de Strasbourg, 11, rue de l'Universite, F-67000, Strasbourg, France; ibata@astro.u-strasbg.fr, martin@newb6.u-strasbg.fr.

[4] Institute for Astronomy, University of Edinburgh, Royal Observatory, Blackford Hill, Edinburgh EH9 3HJ, UK; ferguson@roe.ac.uk.

[5] Institute of Astronomy, Madingley Road, Cambridge CB3 0HA, UK; mike@ast.cam.ac.uk.

[6] Institute of Astronomy, School of Physics, A29, University of Sydney, NSW 2006, Australia; gfl@physics.usyd.edu.au.

[7] Physical Sciences, University of Hertfordshire, Hatfield AL10 9AB, UK; nrt@star.herts.ac.uk.

[8] During the refereeing process of this Letter, Sarajedini et al. (2006) presented strong evidence for the detection of a population of RR Lyrae variable stars in the halo of M33.

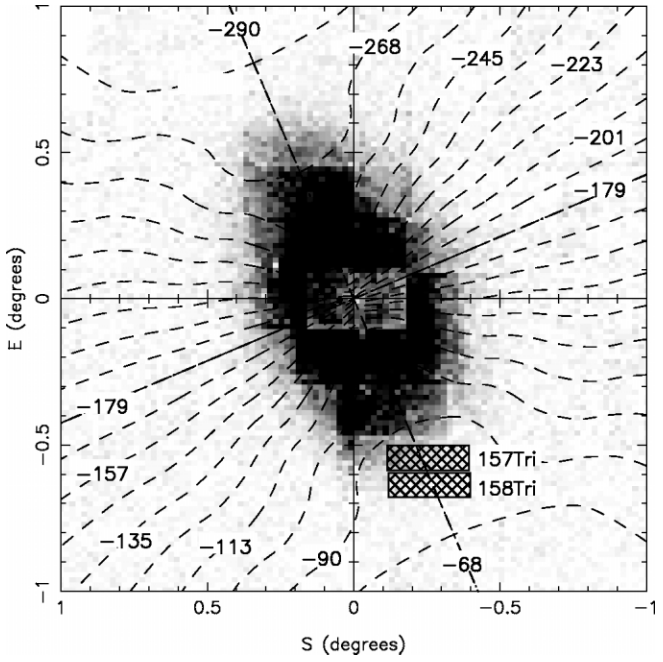

FIG. 1.—Tangent plane projection of RGB stars in M33 with $I < 22$, from our INT WFC survey (Ferguson et al. 2006). The locations of the Keck DEIMOS fields are indicated. Contours show the mean heliocentric radial velocity of a model M33 disk, based on the Corbelli (2003) H I rotation curve.

The contours in Figure 1 show the expected mean stellar heliocentric radial velocities for a kinematic model of M33, based on the H I rotation curve of M33 derived by Corbelli (2003) and shown in her Figure 5. We assume a stellar distribution in M33 described by $\rho\,(R, z) \propto \exp\,(-R/R_e)\,\exp\,(-z/z_e)$, with $R_e = 5.'8$ (1.4 kpc; Regan & Vogel 1994) and $z_e = 0.2$ kpc. Changing z_e within the range [0, 1] kpc makes no significant difference to any of our results. Stars occupy circular orbits with $v_z = 0$ and v_R defined by interpolation of the H I rotation curve, linearly extrapolated beyond $R = 77'$ (18 kpc) where necessary. The model is then corrected for the position angle ($\theta \simeq 23°$) and inclination ($i \simeq 54°$) of the stellar disk of M33. The mean velocity along any sight line through the disk is calculated as $\bar{v}_l = \int \boldsymbol{v}\cdot\hat{\boldsymbol{L}}\rho(R, z)dl / \int \rho(R, z)dl$, and corrected to the heliocentric frame. $\hat{\boldsymbol{L}}$ is a unit vector pointing along the direction of our line of sight.

The data were processed and reduced in the same way as the main M31 survey (Ibata et al. 2005; Chapman et al. 2006). Because of the generally poor observing conditions, the data analyzed here consist of 280 stars with a cross correlation coefficient >0.02, a signal-to-noise ratio in the continuum >2, a Tonry-Davis coefficient (Tonry & Davis 1979) >2, and a velocity error $v_{\rm err} < 25$ km s^{-1} ($\bar{v}_{\rm err} \simeq 10$ km s^{-1}).

3. KINEMATICS

The top two panels of Figure 2 show the heliocentric radial velocity (v_h) distributions in our two fields. The dashed lines indicate $v_h = 0$, and the dot-dashed lines indicate the systemic velocity of M33, $v_h = -179$ km s^{-1}. The dot-dashed histograms show the expected heliocentric velocity distributions of the MW stars that lie in each field using the MW model of Robin et al. (2003) and that satisfy our selection criteria for M33 RGB stars. The histograms have been scaled to match the area of the DEIMOS fields. They show that any contribution from MW foreground stars at $v_h < -80$ km s^{-1} is small for the purposes of this Letter, and so this velocity cut is adopted in the following kinematic analysis. Stars with $v_h > -80$ km s^{-1} are predominantly MW foreground, and the small numbers we observe further suggest that the contamination at more negative velocity will be negligible.

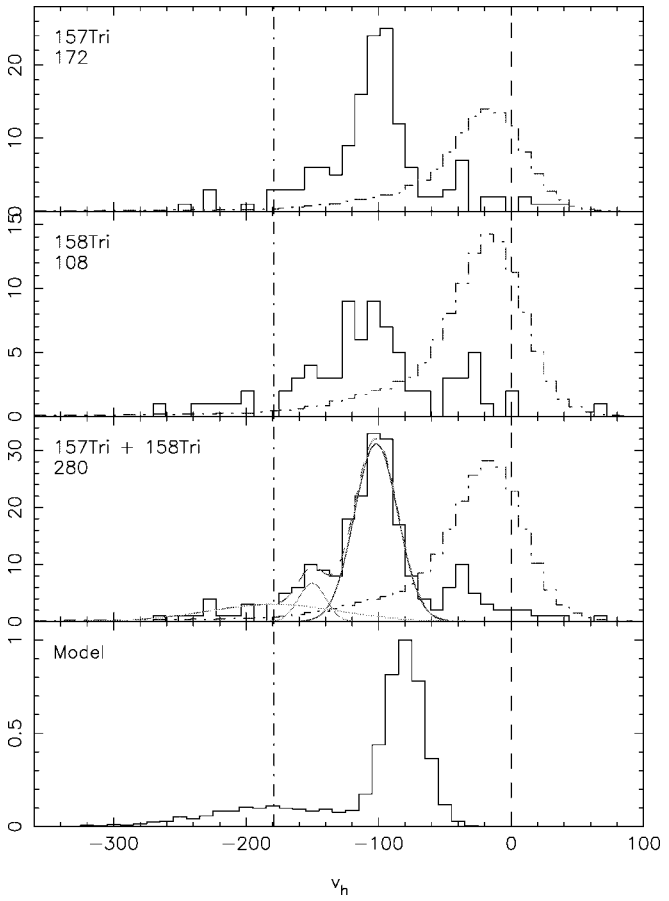

FIG. 2.—*From top to bottom, first and second panels*: Heliocentric radial velocity distributions for our M33 fields. The dashed lines represent zero velocity, and the dot-dashed line represents the systemic velocity of M33, $v_h = -179$ km s^{-1}. The dot-dashed histograms show the heliocentric velocity distribution of the expected MW foreground stars in each field, from the MW model by Robin et al. (2003), which satisfy our color selection criteria. These histograms have been scaled to match the area of the DEIMOS fields, and the small number of stars at $v_h > -80$ km s^{-1}, which are most likely foreground, suggest that contamination at more negative velocity will be negligible. *Third panel*: Same as first two panels, except now the two fields have been added together to boost statistics. Three Gaussian velocity distributions and their summed total are overlaid. See text for details. *Bottom panel*: Expected heliocentric radial velocity distribution of stars in our fields, using our M33 disk model and an additional Gaussian component, representing a smooth stellar halo. [*See the electronic edition of the Journal for a color version of this figure*.]

The third panel of Figure 2 shows the velocity distributions of fields 157 and 158 added together to boost statistics. We expect the main stellar components in M33 will be well fit by individual Gaussians, and any stellar halo component in M33 will have a velocity distribution centered on $v_h = -179$ km s^{-1}. Since M33 is ~10 times less massive than M31, we expect that the M33 halo velocity dispersion will be $\sim 10^{1/2}$ that of M31 ($\sigma_{\rm M31} \sim$ 145 km s^{-1}; Chapman et al. 2006). The broad Gaussian overlaid in the third panel of Figure 2 represents a M33 halo component with a dispersion of $\sigma = 50$ km s^{-1}, scaled to match the approximate number of stars observed. We also expect that the prominent peak of stars in these fields is due to the dominant disk of M33. Therefore, we have subtracted the halo Gaussian

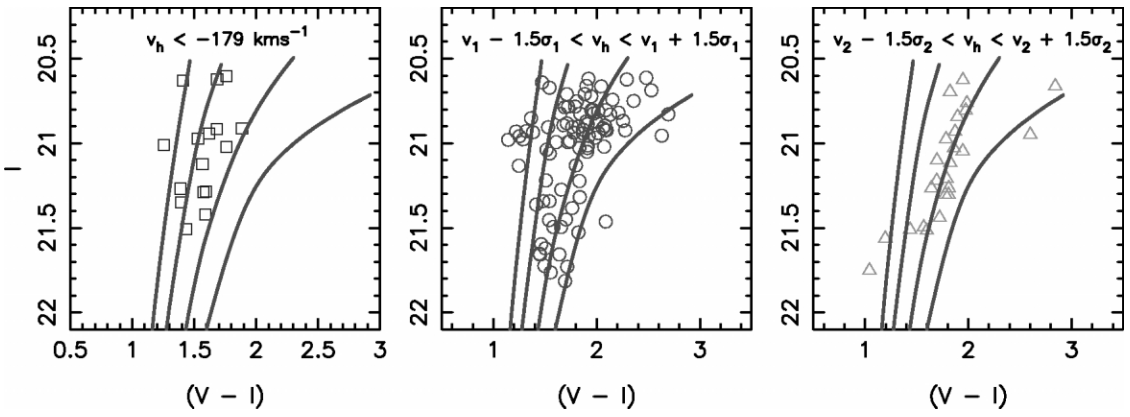

FIG. 3.—CMDs of spectroscopically observed RGB stars from fields 157 and 158, selected to satisfy the velocity cuts indicated ($\sigma_1 = 16$ km s^{-1}, $\sigma_2 = 10$ km s^{-1}). These velocity cuts predominantly sample stars which belong to the candidate halo (*left*), disk (*middle*) and the third component (*right*). Victoria-Regina isochrones (VandenBerg et al. 2006), corresponding to 13 Gyr old stars and with metallicities of [Fe/H] = −2.0, −1.3, −0.8, and −0.5, are overlaid. [*See the electronic edition of the Journal for a color version of this figure*.]

from the v_h distribution in the third panel and fitted a Gaussian to this peak, centered at $v_1 = -102 \pm 2$ km s^{-1} with an uncorrected dispersion $\sigma_1 = 16 \pm 3$ km s^{-1} (corrected dispersion of ∼12.5 km s^{-1}). The residuals of this fit show a prominent grouping of stars at $v \sim -150$ km s^{-1}. We fit a third Gaussian to this feature, with a peak $v_2 = -150 \pm 4$ km s^{-1} and a dispersion $\sigma_2 = 10 \pm 4$ km s^{-1}. The latter quantity is more poorly constrained than is given by the formal error, however, as its dispersion is covariant with the dispersion of the disk and halo, which have been fitted independently. All three Gaussians and their summed total are overlaid in the third panel of Figure 2.

The bottom panel of Figure 2 shows the expected distribution of stars at the positions of fields 157 and 158 for the model of M33 shown in Figure 1 combined with a halo model with a radial velocity dispersion of 50 km s^{-1}. The radial velocity dispersion of the disk is set to 16 km s^{-1}, to mimic our observations. The normalization of both components is chosen to approximately match the corresponding peaks in the data. A comparison between model and data shows (1) the peak at $v_2 = -150$ km s^{-1} does not naturally arise as a result of our line of sight through the main M33 disk sampling stars at different circular velocities, and (2) the stellar disk is offset in v_h from the H I disk by ∼20–25 km s^{-1}, implying a deprojected offset of ∼25–30 km s^{-1}. For comparison, the asymmetric drift between the stars and H I in the MW and M31 is of order 15–20 km s^{-1}. Scaling for mass, the expected asymmetric drift in M33 is not likely to be more than ∼10 km s^{-1}. We believe that the velocity offset between the two disks is due to differential warping, specifically that the H I disk is warping into our line of sight at large radius from M33. This has been implied, quite spectacularly, by Rogstad et al. (1976; see their Fig. 14), and is consistent with the magnitude of the velocity offset.

4. METALLICITIES

Figure 3 shows the color-magnitude diagrams (CMDs) for the spectroscopically observed M33 RGB stars in fields 157 and 158, divided by the radial velocity cuts indicated so as to kinematically separate the three candidate components as best as possible. Victoria-Regina isochrones from VandenBerg et al. (2006), with *BVRI* color-$T_{\rm eff}$ relations as described by VandenBerg & Clem (2003), corresponding to a 13 Gyr stellar population with metallicities of [Fe/H] = −2.0, −1.3, −0.8, and −0.5, are also overlaid.

The differences between the CMDs in Figure 3 are striking and appear to validate our kinematic deconvolution. The candidate M33 halo stars are predominantly bluer and have a smaller color dispersion than the candidate disk stars, indicating a difference in the age and/or metallicity properties of the populations. Assuming both populations are 13 Gyr old implies a median photometric metallicity for the halo of [Fe/H] = −1.3 ± 0.1, with a dispersion of $\sigma_{\rm [Fe/H]} = 0.21$. Given the small number of stars that contribute to this measurement, this is consistent with the A. Ferguson et al. (2006, in preparation) metallicity measurement for the halo, of [Fe/H] = −1.5 ± 0.1. The disk has an implied photometric metallicity of [Fe/H] = −0.9 ± 0.1 and a broader dispersion of $\sigma_{\rm [Fe/H]} = 0.35$. The median color (metallicity) of the "third component" is similar to the disk, although its color dispersion is remarkably narrow ($\sigma_{\rm [Fe/H]} = 0.15$). This population is difficult to isolate kinematically, and our sample could be contaminated by both of the other two components. However, the locus of its stars on the CMD does not clearly associate it with either the candidate disk or halo population and is reminiscent of a CMD for a single stellar population. If this population was due to MW foreground contamination, we would not expect its stars to occupy so well defined a locus in this diagram. The most probable explanation is that these stars belong to a stellar stream. These stars do not, however, define a spatially obvious structure, but given our limited field size and that our choice of slitlet position will affect the spatial distribution, this test is inconclusive at best.

We calculate the spectroscopic metallicity of the halo stars by measuring the equivalent width of the CaT from stacked spectra, using a method identical to that used in Ibata et al. (2005) and Chapman et al. (2006). We find that [Fe/H] = −1.5 ± 0.3, in good agreement with the photometric measurement. The large uncertainty reflects the relatively low signal-to-noise ratio of the stacked spectrum. We are unable to measure the metallicities of the other two components in this way, since their velocities cause the CaT to lie on top of strong sky lines, which prevents accurate equivalent width measurements.

5. DISCUSSION

M33 is considered an example of the quintessential disk galaxy, with no evidence for any bulge or spheroid component. However, the radial profile for M33 presented in A. Ferguson et al. (2006, in preparation), based on our INT WFC observations, reveals for the first time the presence of a spatially extended, low-density component. Using Keck DEIMOS, we

have identified a population of RGB stars that have velocities centered on the systemic velocity of M33 and that appear to have a large dispersion ($\sigma \sim 50$ km s^{-1}). These stars are bluer than other RGB stars in M33 with a small color dispersion. Their average metallicity is [Fe/H] ~ -1.5, and we attribute them to the newly discovered halo component of M33. The halos of the MW and M31 have similar metallicities to this (Eggen et al. 1962; Chapman et al. 2006; Kalirai et al. 2006), even though both these galaxies are ~10 times more massive than M33. It is important to emphasize that there is no evidence of a trend linking halo metallicity to galaxy mass or luminosity for the Local Group galaxies, as has been suggested from recent *Hubble Space Telescope* studies of galaxies within ~10 Mpc (Mouhcine et al. 2005a, 2005b). Instead, all the large Local Group spiral galaxies appear to have very similar halo metallicities.

We also observe stars in the disk of M33. Their v_h distribution is well described by a Gaussian with an uncorrected dispersion of $\sigma \simeq 16$ km s^{-1}, corresponding to a corrected dispersion of $\simeq$12.5 km s^{-1}. These stars are redder and have a broader color dispersion than the halo stars. The stellar disk is offset in v_h from the H I disk in our simple model by ~20–25 km s^{-1}, which is fully consistent with the extreme warping of the H I disk implied by Rogstad et al. (1976).

Finally, we present evidence for a third kinematic feature in M33, revealed by the v_h distribution of the southern fields. The velocity dispersion of this component is not well constrained by our data. A comparison to our simple model of the disk of M33 shows that this feature does not arise as a result of our line of sight through M33 sampling stars at different circular velocities in the main disk. The locus of these stars in the CMD has a remarkably small color dispersion, reminiscent of a single stellar population and inconsistent with belonging to a foreground population. We believe the most likely explanation for this feature is that it is a stellar stream. However, more spectroscopic observations of fields at different locations around the disk of M33 are required before the true nature of this intriguing feature is revealed.

The data presented herein were obtained at the W. M. Keck Observatory, which is operated as a scientific partnership among the California Institute of Technology, the University of California, and the National Aeronautics and Space Administration. The Observatory was made possible by the generous financial support of the W. M. Keck Foundation. We thank E. Corbelli for supplying us with her data for the H I rotation curve of M33 and the anonymous referee for constructive comments. A. W. M. would like to thank J. Navarro and S. Ellison for financial support. A. M. N. F. is supported by a Marie Curie Excellence grant from the European Commission under contract MCEXT-CT-2005-025869. G. F. L. acknowledges support through ARC DP0343508.

REFERENCES

Bothun, G. D. 1992, AJ, 103, 104
Chandar, R., Bianchi, L., Ford, H. C., & Sarajedini, A. 2002, ApJ, 564, 712
Chapman, S. C., Ibata, R., Lewis, G. F., Ferguson, A. M. N., Irwin, M., McConnachie, A., & Tanvir, N. 2005, ApJ, 632, L87
———. 2006, ApJ, submitted (astro-ph/0602604)
Corbelli, E. 2003, MNRAS, 342, 199
de Vaucouleurs, G. 1959, ApJ, 130, 728
Dressler, A., & Richstone, D. O. 1988, ApJ, 324, 701
Eggen, O. J., Lynden-Bell, D., & Sandage, A. R. 1962, ApJ, 136, 748
Faber, S. M., et al. 2003, in SPIE Proc., 4841, 1657
Ferguson, A., Irwin, M., Chapman, S., Ibata, R., Lewis, G., & Tanvir, N. 2006, preprint (astro-ph/0601121)
Genzel, R., Eckart, A., Ott, T., & Eisenhauer, F. 1997, MNRAS, 291, 219
Ibata, R., Chapman, S., Ferguson, A. M. N., Irwin, M., Lewis, G., & McConnachie, A. 2004, MNRAS, 351, 117
Ibata, R., Chapman, S., Ferguson, A. M. N., Lewis, G., Irwin, M., & Tanvir, N. 2005, ApJ, 634, 287
Kalirai, J. S., et al. 2006, ApJ, in press (astro-ph/0605170)
Kormendy, J. 1988, ApJ, 325, 128
Kormendy, J., & McClure, R. D. 1993, AJ, 105, 1793
Lauer, T. R., Faber, S. M., Ajhar, E. A., Grillmair, C. J., & Scowen, P. A. 1998, AJ, 116, 2263
McConnachie, A. W., Irwin, M. J., Ferguson, A. M. N., Ibata, R. A., Lewis, G. F., & Tanvir, N. 2004a, MNRAS, 350, 243
———. 2005, MNRAS, 356, 979
McConnachie, A. W., Irwin, M. J., Lewis, G. F., Ibata, R. A., Chapman, S. C., Ferguson, A. M. N., & Tanvir, N. R. 2004b, MNRAS, 351, L94
McLean, I. S., & Liu, T. 1996, ApJ, 456, 499
Minniti, D., Olszewski, E. W., & Rieke, M. 1993, ApJ, 410, L79
Mouhcine, M., Ferguson, H. C., Rich, R. M., Brown, T. M., & Smith, T. E. 2005a, ApJ, 633, 821
Mouhcine, M., Rich, R. M., Ferguson, H. C., Brown, T. M., & Smith, T. E. 2005b, ApJ, 633, 828
Regan, M. W., & Vogel, S. N. 1994, ApJ, 434, 536
Robin, A. C., Reylé, C., Derrière, S., & Picaud, S. 2003, A&A, 409, 523
Rogstad, D. H., Wright, M. C. H., & Lockhart, I. A. 1976, ApJ, 204, 703
Sarajedini, A., Barker, M. K., Geisler, D., Harding, P., & Schommer, R. 2006, preprint (astro-ph/0605580)
Tonry, J., & Davis, M. 1979, AJ, 84, 1511
VandenBerg, D. A., Bergbusch, P. A., & Dowler, P. D. 2006, ApJS, 162, 375
VandenBerg, D. A., & Clem, J. L. 2003, AJ, 126, 778